



AIAA-93-3369

**A Projection Method for Combustion in
the Zero Mach Number Limit**

M. Lai and P. Colella
University of California, Berkeley
Berkeley, CA

J. Bell
Lawrence Livermore National Laboratory
Livermore, CA

**11th AIAA
Computational Fluid Dynamics Conference
July 6-9, 1993 / Orlando, FL**

A Projection Method for Combustion in the Zero Mach Number Limit

Mindy Lai*

*University of California, Berkeley
Berkeley, CA 94720*

John B. Bell**

*Lawrence Livermore National Laboratory
Livermore, CA 94550*

Phillip Colella***

*University of California, Berkeley
Berkeley, CA 94720*

Abstract

We present a finite difference method for solving the equations of combustion in the limit of zero Mach number. In this limit, acoustic waves are weak and do not contribute significantly to the fluid dynamics or energetics. For the equations describing this limit, we construct an efficient, high-resolution numerical method that allows for large temperature and density variations and correctly accounts for expansion due to heat release. The method, a projection method, is a second order fractional step scheme. In the first step, we compute the solution to advection-reaction-diffusion equations for the velocity, temperature, and species. In the second step, we impose the constraint on the divergence of the velocity field that represents the effect of bulk compression and expansion of the fluid due to heat release. We demonstrate our method on the problem of combustion in an enclosed container.

Nomenclature

c_p	specific heat
i, j	spatial indices
k	reaction rate
n	time index
p	perturbational pressure
q_0	heat release coefficient
t	time
$\mathbf{u} = (u, v)$	velocity
D_0	central difference divergence operator

G_0	central difference gradient operator
\mathbf{I}	identity operator
L^h	discrete viscous operator
M	Mach number
P	pressure
P_0	bulk thermodynamic pressure
\mathbf{P}	projection operator
Pr	Prandtl number
R	ideal gas constant
Re	Reynolds number
Sc	Schmidt number
T	temperature
$U_{ij} = (u_{ij}, v_{ij})$	discrete velocity
Z	mass fraction
\mathcal{D}	coefficient of species diffusion
κ	coefficient of thermal diffusion
ρ	density
γ	ratio of specific heats
μ	absolute viscosity
Ω	spatial domain
σ	CFL number
Δ^h	standard five point Laplacian
L_p^h	five pt variable coefficient operator
Δx	mesh spacing in the x direction
Δy	mesh spacing in the y direction

Introduction

In this paper we present a numerical method for solving a system of equations describing combustion in the zero Mach number limit. This limiting system was first developed for inviscid flow by Baum and Rehm[8] and later extended to viscous flow by Majda and Sethian[7]. In this limit, the acoustic waves are fast and weak, and they do not contribute significantly to the fluid dynamics.

The starting point for the derivation of the limiting set of equations is the following scaling behavior for

*Graduate student, Dept. of Mechanical Engineering, student member AIAA

**Group Leader, Applied Mathematics Group, member AIAA

***Professor, Dept. of Mechanical Engineering, member AIAA

Copyright © 1993 by Mindy Lai. Published by the American Institute of Aeronautics and Astronautics, Inc. with permission.

pressure.

$$P(x, t) = P_0(t) + p(x, t) \quad (1.1)$$

$$\frac{p(x, t)}{P_0(t)} = O(M^2)$$

The two terms, P_0 and p , have physical significance: P_0 is the bulk thermodynamic pressure which varies in time only, while the gradient of p is the pressure gradient term in the momentum equation.

For simplicity, we make several assumptions about our system. We first assume that single step chemistry exists (that is, reactants go to products irreversibly.) We use an Arrhenius reaction rate model, and take all diffusion coefficients to be constant. We also assume reactants and products have the same molecular weight. All assumptions are made for ease of computation; nothing inherent in the method prevents more complicated models from being used.

Given these simplifying assumptions, our system of equations for combustion in a closed container, based on those in [7], take the form

$$\rho \frac{D\mathbf{u}}{Dt} = -\nabla p + \mu \nabla \cdot \left(\frac{1}{2} (\nabla \mathbf{u} + (\nabla \mathbf{u})^T) \right) \quad (1.2)$$

$$\rho c_p \frac{DT}{Dt} = \frac{dP_0}{dt} + \kappa \Delta T + q_0 k \rho Z \quad (1.3)$$

$$\rho \frac{DZ}{Dt} = \mathcal{D}(\nabla \cdot \rho \nabla Z) - k \rho Z \quad (1.4)$$

$$\rho = P_0 / (RT) \quad (1.5)$$

$$\frac{dP_0}{dt} = \frac{(\gamma - 1)}{\text{vol}(\Omega)} \int_{\Omega} (q_0 k \rho Z + \kappa \Delta T) d\Omega \quad (1.6)$$

$$\nabla \cdot \mathbf{u} = \frac{-dP_0/dt + (\gamma - 1) (q_0 k \rho Z + \kappa \Delta T)}{\gamma P_0} \quad (1.7)$$

where equations (1.2), (1.3) and (1.4) are conservation equations for momentum, energy, and species, respectively, (1.5) is the ideal gas equation of state, (1.6) is the evolution equation for bulk thermodynamic pressure, and (1.7) is the divergence constraint on the velocity. Z , the mass fraction is defined as the ratio of unburned mass to total mass.

Note that there is no explicit density equation to be solved. Instead, conservation of mass is used to derive the divergence constraint (1.7), given that the energy equation (1.3), the equation of state (1.5), and the ordi-

nary differential equation for the thermodynamic pressure is satisfied. The divergence equation (1.7) represents the extent to which the flow is compressible. Despite the fact that energy is released and the fluid expands only locally along the flame front, the time derivative of P_0 contributes a uniform background to the volume source representing the bulk compression of the fluid to compensate for the expansion along the flame front.

We solve the system using a modified projection method. Projection methods were first introduced by Chorin[4] to solve the Navier-Stokes equations for incompressible flow. The fractional step method he proposed involves first advancing the advection-diffusion equation in time to find an intermediate velocity field and then, in turn, projecting this field onto the space of divergence free vector fields.

Chorin's original method was first order in time and second order in space. Various investigators have extended the projection method to full second order accuracy including Van Kan[9], Bell, Colella, and Glaz[1] and Bell, Colella, and Howell[2]. Bell and Marcus[3] applied the method to variable density flow. Here, we extend the approach in [1],[2] and [3] to solve the system of equations for reacting flow in the zero Mach number limit. The major difference is that the flow is no longer incompressible and our divergence constraint is no longer homogeneous. We are required to modify the projection to account for the non-zero right hand side of (1.7).

Specifically, the incompressible projection is based on the decomposition of an arbitrary vector field into its gradient and divergence-free parts

$$\mathbf{W} = \mathbf{V}^d + \nabla \phi \quad (1.8)$$

$$\nabla \cdot \mathbf{V}^d = 0$$

where the normal component of \mathbf{V}^d vanishes on the boundary of the domain. \mathbf{V}^d is related to vortical motions while the scalar potential, $\nabla \phi$, is related to the pressure gradient. In the present case, we further split the gradient into two parts.

$$\mathbf{W} = \mathbf{V}^d + \nabla \phi + \nabla \psi \quad (1.9)$$

where \mathbf{V}^d is still related to vorticity generation and $\nabla \phi$ is still associated with the pressure, but we have an additional gradient, $\nabla \psi$, which accounts for the volume sources in (1.7) and is part of the velocity field:

$$\mathbf{u} = \mathbf{V}^d + \nabla \psi \quad (1.10)$$

The procedure for solving the equations for low Mach number reacting flow is similar to that used for solving the equations for incompressible flow, modulo

the required additions to solve the scalar equations for temperature, pressure, density and mass fraction. The first step is to calculate all non-linear advective terms using a Godunov procedure. This procedure is second order accurate for smooth flow, stable at discontinuities, and has been shown to provide excellent resolution for flows with complex vortical structure. The Godunov method works by tracing backward along characteristics to determine the conservative flux that entered (or exited) each of the finite difference cell's surfaces. These fluxes are then used to construct the advective terms. We use this method to calculate flux terms for velocity, energy, and species (mass fraction.)

Next, we update temperature and mass fraction by using a Crank-Nicolson discretization where all source terms are approximated at time $t^{n+1/2}$. We use these updated quantities to find bulk pressure by performing the integration indicated in (1.6), and use the result to update density using the equation of state (1.5). Once all these updates have been performed, we re-evaluate all volume sources at time $t^{n+1/2}$.

We continue by finding an approximation to the updated velocity field by solving a Crank-Nicolson discretization of the momentum equation where the pressure term is treated as a source and evaluated at time $t^{n+1/2}$. Finally, we complete the velocity update by performing the projections to enforce the compressibility constraint. At this time we also calculate the updated perturbational pressure.

In the next section, we provide details on the Godunov procedure for computing the time centered approximations to the non-linear flux terms. We follow this discussion with details on solving the scalar equation. Next, we outline our time-stepping strategy and discuss the projection. Finally, we present some results for the problem of combustion in a closed container.

Treatment of Non-Linear Terms

This section discusses the steps taken to calculate the time-centered non-linear terms. The Godunov procedure is a conservative, second-order accurate method similar to that used by [2]. It is a multistep method whereby we first predict values at cell edges at time $t^{n+1/2}$ using Taylor series extrapolation, upwind at cell edges, enforce the divergence constraint on the predicted velocities, and then use the predicted quantities to construct non-linear terms. Cell centers are located at (i,j) , the right side of each cell is at $i+1/2$ and the top is at $j+1/2$. We define velocity, pressure, temperature, density, and mass fraction at cell centers.

The algorithm for finding the velocity advective terms in two space dimensions is presented here in detail. The scalar advective terms for temperature and

mass fraction are calculated in an analogous manner.

To extrapolate to each of the four cell edges, we use the Taylor series approximations

$$U_{i+1/2,j}^{n+1/2,L} = U_{i,j}^n + \frac{\Delta x}{2} U_{x,ij}^n + \frac{\Delta t}{2} U_{t,ij}^n \quad (2.1)$$

$$U_{i-1/2,j}^{n+1/2,R} = U_{i,j}^n - \frac{\Delta x}{2} U_{x,ij}^n + \frac{\Delta t}{2} U_{t,ij}^n \quad (2.2)$$

$$U_{i,j+1/2}^{n+1/2,T} = U_{i,j}^n + \frac{\Delta y}{2} U_{y,ij}^n + \frac{\Delta t}{2} U_{t,ij}^n \quad (2.3)$$

$$U_{i,j-1/2}^{n+1/2,L} = U_{i,j}^n - \frac{\Delta y}{2} U_{y,ij}^n + \frac{\Delta t}{2} U_{t,ij}^n \quad (2.4)$$

where the spatial derivatives are estimated by the fourth-order monotonicity limited slopes used by [2]. These slopes were selected in favor of the van Leer limited slopes used in [1] because they have slightly less damping.

The differential equation is substituted into the expressions above to eliminate the temporal derivative, but the pressure terms are omitted. As in [2], we will correct for the pressure using a separate pressure calculation. Thus (2.1) becomes

$$U_{i+1/2,j}^{n+1/2,L} = U_{i,j}^n + \left(\frac{\Delta x}{2} - u_{i,j} \frac{\Delta t}{2} \right) U_{x,ij} - \frac{\Delta t}{2} \left((vU_y)_{i,j} - \frac{\mu}{\rho_{i,j}} (L^h U)_{i,j} \right) \quad (2.5)$$

Slopes in the normal directions are replaced by fourth-order approximations, while slopes in the transverse direction are calculated by

$$(vU_y)_{i,j} = \begin{cases} v_{i,j} \cdot \frac{(U_{i,j} - U_{i,j-1})}{\Delta y} & \text{if } (v_{i,j} > 0) \\ v_{i,j} \cdot \frac{(U_{i,j+1} - U_{i,j})}{\Delta y} & \text{if } (v_{i,j} \leq 0) \end{cases} \quad (2.6)$$

The next step in the method is to resolve the ambiguity at cell edges by selecting one of the two extrapolated values. Recall that at each cell edge, two values have been extrapolated, one from the left and one from the right (or one from the top and another from the bottom.) Selecting a single value from these two is done by solving a Riemann problem. The solution is shown here for the velocity at the right cell edge. Dropping the time index, we find the normal component

$$u_{i+1/2,j} = \begin{cases} u^L & \text{if } \frac{u_{i,j} + u_{i+1,j}}{2} \geq 0 \\ u^R & \text{otherwise} \end{cases} \quad (2.7)$$

Then we use the normal velocity to find the tangential component

$$v_{i+1/2,j} = \begin{cases} v^L & \text{if } u_{i+1/2,j} > 0 \\ v^R & \text{if } u_{i+1/2,j} < 0 \\ \frac{1}{2}(v^L + v^R) & \text{if } u_{i+1/2,j} = 0 \end{cases} \quad (2.8)$$

We continue by enforcing the divergence constraint on these predicted velocities we've just calculated using a MAC type projection modified for variable density flow. The projection is based on the idea that the predicted velocities can be decomposed into two components, one divergence-free and the other the gradient of a scalar. The gradient piece has two factors contributing to it: it encompasses both the pressure gradient and a second gradient associated with the heat released from combustion. Specifically, if we write the predicted velocities as

$$U^{n+1/2} = U^d + \nabla\phi + \nabla\psi \quad (2.9)$$

we can take the divergence of (2.7) to form the Poisson equation

$$\Delta\phi = \nabla \cdot U - \Delta\psi \quad (2.10)$$

and solve it for the scalar field, ϕ . From ϕ , we can construct $\nabla\phi$ and recover both the pressure gradient and the velocities which satisfy the divergence constraint using (2.9). This is a particularly straightforward process, since we are given the velocities at cell edges. This enables us to use the MAC centering (Harlow and Welch [6]) of velocities and pressures in discretizing (2.10).

In detail, we calculate the MAC divergence at cell centers

$$(D^M U)_{i,j} = \frac{1}{\Delta x} (u_{i+1/2,j} - u_{i-1/2,j}) + \frac{1}{\Delta y} (v_{i,j+1/2} - v_{i,j-1/2}) \quad (2.11)$$

and approximate the volume source term at cell centers

$$S_{i,j} = \frac{1}{\gamma P_0} \left(-\frac{dP_0}{dt} + (\gamma - 1)(\kappa\Delta T + q_0 k\rho Z) \right)_{i,j} \quad (2.12)$$

where the solution is evaluated at time step n , and the derivative of the thermodynamic pressure is obtained by summing the remaining terms over the grid, and dividing by the area. We subtract the source term from the MAC divergence, and use it as a right hand side in solving the Poisson equation with variable coefficients

below. Cell centered Neumann boundaries are used.

$$(L^h_p U)_{i,j} = \frac{1}{\Delta x^2} \left(\frac{(\phi_{i+1,j} - \phi_{i,j})}{P_{i+1/2,j}} - \frac{(\phi_{i,j} - \phi_{i-1,j})}{P_{i-1/2,j}} \right) + \frac{1}{\Delta y^2} \left(\frac{(\phi_{i,j+1} - \phi_{i,j})}{P_{i,j+1/2}} - \frac{(\phi_{i,j} - \phi_{i,j-1})}{P_{i,j-1/2}} \right) = (D^M U)_{i,j} - S_{i,j} \quad (2.13)$$

Once we have obtained ϕ , we compute the gradient to be used as a pressure correction and correct the predicted velocities

$$\frac{\Delta t}{2} P_{x,i+1/2,j} = \frac{(\phi_{i+1,j} - \phi_{i,j})}{\Delta x}$$

$$\frac{\Delta t}{2} P_{y,i+1/2,j} = \frac{(\phi_{i,j+1} + \phi_{i,j+1} - \phi_{i,j-1} - \phi_{i,j-1})}{4\Delta y}$$

$$U_{i+1/2,j}^{n+1/2} \leftarrow U_{i+1/2,j}^{n+1/2} - \begin{pmatrix} \frac{\Delta t}{2} P_{x,i+1/2,j} \\ \frac{\Delta t}{2} P_{y,i+1/2,j} \end{pmatrix}$$

Thus $U^{n+1/2}$ satisfies a suitably accurate approximation to $U^{n+1/2} = U^d + \nabla\psi$ where $\Delta\psi = S$ and $\nabla \cdot U^d = 0$. We also note that the choice of discrete approximation to dP_0/dt guarantees that the equation (2.13) is solvable, since the appropriate discrete average of the right-hand side over the domain is zero.

Finally, we use these U 's to construct the non-linear terms $[(U \cdot \nabla) U]^{n+1/2}$ using centered differencing

$$uU_x + vU_y = \frac{1}{2} (u_{i+1/2,j} - u_{i-1/2,j}) \frac{(U_{i+1/2,j} - U_{i-1/2,j})}{\Delta x} + \frac{1}{2} (v_{i,j+1/2} - v_{i,j-1/2}) \frac{(U_{i,j+1/2} - U_{i,j-1/2})}{\Delta y} \quad (2.15)$$

We need to use a slightly modified version of the predictor in calculating the advection terms for mass fraction. We observed that using the algorithm above introduced a mild non-linear instability for CFL numbers greater than about .5 in the reacting flow case. Using the following alternative scheme alleviates the problem.

First calculate

$$\tilde{Z} = Z + \left(\frac{\Delta t - \tau}{2} \right) (\mathcal{D}\Delta^h Z - kZ) \quad (2.16)$$

where $\tau = \min(h^2/(8\mathcal{D}), \Delta t)$. Next, calculate

$$\bar{Z} = \tilde{Z} + \frac{\tau}{2} \mathcal{D}\Delta^h \tilde{Z} - \frac{\tau}{2} k\tilde{Z} \quad (2.17)$$

and use these intermediate values in the extrapolation step

$$Z_{i+1/2,j}^{n+1/2,L} = \bar{Z}_{i,j}^n + \left(\frac{\Delta x}{2} - u_{i,j} \frac{\Delta t}{2}\right) Z_{x,u} - \frac{\Delta t}{2} (vU_y)_{i,j} \quad (2.18)$$

Essentially, what we are doing with this modified algorithm is smoothing the source terms that come from the chemical reaction by performing one point-Jacobi iteration. The smoothing is consistent with the governing differential equation and introduces no loss of accuracy.

Since the Godunov scheme is explicit, we need to satisfy a CFL condition on the time step to insure stability. This constraint is

$$\Delta t \leq \sigma \min \left(\frac{\Delta x_{i,j}}{|u_{i,j}^n|}, \frac{\Delta y_{i,j}}{|v_{i,j}^n|} \right) \quad (2.19)$$

$$\sigma \leq 1$$

Scalar Updates

After the Godunov procedure, we are almost in a position to update mass fraction by solving a Crank-Nicolson discretization of the species conservation equation (1.4). First, however, we require that all source terms be evaluated at $t^{n+1/2}$. All that is needed is a time-centered approximation of T ; we use a Taylor series to make the necessary guess. We then solve

$$\rho^{n+1/2} \left(\frac{Z^{n+1} - Z^n}{\Delta t} + [(\mathbf{u} \cdot \nabla) Z]^{n+1/2} \right) = \mathcal{D}(\rho^{n+1/2} G \left(\frac{Z^{n+1} + Z^n}{2} \right)) - (k\rho)^{n+1/2} \left(\frac{Z^{n+1} + Z^n}{2} \right) \quad (3.1)$$

for Z^{n+1} using multigrid, and average mass fraction at the old and new times to get a good approximation for $Z^{n+1/2}$.

We perform a similar process for updating temperature by solving the discretized energy equation (1.3)

$$\rho^{n+1/2} c_p \left(\frac{T^{n+1} - T^n}{\Delta t} + [(\mathbf{u} \cdot \nabla) T]^{n+1/2} \right) = \kappa \Delta^h \left(\frac{T^{n+1} + T^n}{2} \right) + \left(\frac{dP_0}{dt} \right)^{n+1/2} + (q_0 k\rho Z)^{n+1/2} \quad (3.2)$$

As with mass fraction, we average temperature at the old and new times to obtain a good estimate for $T^{n+1/2}$.

We continue by integrating the evolution equation for bulk thermodynamic pressure (1.6). We use the results of this integration to calculate a corrected value for $(DP_0/Dt)^{n+1/2}$ and P_0^{n+1} which are used, in turn, to

update density and evaluate the volume source terms at time $(n+1)\Delta t$.

Projection

The projection step of the algorithm serves to enforce the divergence constraint (1.7) and enables us to find updates for velocity and perturbational pressure. The mechanics of this projection are identical to those of the MAC projection: we take the divergence of the vector field we're projecting; solve the Poisson equation for the scalar field, ϕ ; and use the scalar field to find $\mathbf{V}^d + \nabla\psi$, the velocity update, and the pressure update.

The two questions we address in this section are

a) How do we enforce the divergence constraint as a function of time?

b) What is the spatial discretization of the constraint?

In response to the first question, we use a second-order predictor-corrector algorithm in [1] to intertwine the viscous operator and the constraint. We first compute U^* , an approximation to U^{n+1} , by solving

$$\frac{U^* - U^n}{\Delta t} + [(\mathbf{U} \cdot \nabla) \mathbf{U}]^{n+1/2} = -\frac{1}{\rho^{n+1/2}} G p^{n-1/2} + \frac{\mu}{\rho^{n+1/2}} L^h \left(\frac{U^* + U^n}{2} \right) \quad (4.1)$$

and then use U^* in our decomposition. This decomposition is based on the relationship

$$\frac{U^{n+1} - U^n}{\Delta t} + \frac{1}{\rho^{n+1/2}} G p^{n+1/2} = \frac{U^* - U^n}{\Delta t} + \frac{1}{\rho^{n+1/2}} G p^{n-1/2} = -[(\mathbf{U} \cdot \nabla) \mathbf{U}]^{n+1/2} + \frac{\mu}{\rho^{n+1/2}} L^h \left(\frac{U^* + U^n}{2} \right) \quad (4.2)$$

which can be rewritten as

$$\frac{U^{n+1} - U^n}{\Delta t} + \frac{G\delta^{n+1/2}}{\rho^{n+1/2}} = \frac{U^* - U^n}{\Delta t} \quad (4.3)$$

where $\delta = p^{n+1/2} - p^{n-1/2}$.

As in the MAC case, we satisfy the divergence constraint by subtracting velocity source terms from the divergence of the right hand side. That is, we solve

$$\nabla_u \cdot \frac{1}{\rho} \nabla \delta = D \left(\frac{U^* - U^n}{\Delta t} \right) - S \quad (4.4)$$

where $S = ((DU)^{n+1} - (DU)^n) / (\Delta t)$ to be consistent with the time centering of the projection.

The question remains as to what spatial discretization to use for (4.6). Unlike in the predictor step, the velocities are all centered at the same points on the grid, so that the choice is not straightforward. We use a hybrid formulation with an additional filter to remove modes that are left in by the projection. Specifically, in the primary projection, we solve

$$\Delta_p^h \delta = D_0 \left[\frac{U^* - U^n}{\Delta t} \right] - \left[\frac{S^{n+1} - S^n}{\Delta t} \right] \quad (4.5)$$

To update the perturbational pressure and calculate \bar{U} , an intermediate velocity field, we use

$$\bar{U} = U^n - \frac{\Delta t}{\rho^{n+1/2}} G_0 \delta \quad (4.6)$$

$$G_0 p^{n+1/2} = G_0 \delta + G_0 p^{n-1/2} \quad (4.7)$$

Next, we solve (4.8)

$$\Delta^h \psi = \frac{1}{\gamma P_0} \left(-\frac{dP_0}{dt} + (\gamma - 1) (\kappa \Delta T + q_0 k p Z) \right)^{n+1}$$

and construct $G_0 \psi$. To remove non-physical high-frequency modes that persist after the primary projection, we construct a "filter" consisting of one point-Jacobi iteration of a diagonal - five point discretization of the Laplacian, and apply it to $\bar{U} - G_0 \psi$ [10]. Finally, we update velocity by adding $G_0 \psi$ to the filtered field.

Note that by using this approach we do not strictly enforce the divergence constraint in that $D_0 U^{n+1} \neq \Delta^h \psi$. The algorithm does, however, appear to be numerically accurate and stable as demonstrated in the last section.

Results

Below some results of our calculations are shown and convergence is demonstrated for the method discussed in the previous sections. Initially, we define a smooth initial velocity profile inside a unit square with homogeneous Dirichlet boundary conditions. The initial temperature profile consists of two smooth "hot spots" in the lower left and upper right corners, corresponding to areas where the fluid contains only products of combustion. The remainder of the fluid consists of low temperature reactants. The temperature in these hot areas is great enough to set off the ignition temperature kinetics. The Reynolds number is approximately 5000. Plots are shown at both early and later times.

We note especially the complex vortical structure that forms in the burnt gas due to the baroclinic generation of vorticity at the flame front and the enhanced mixing of the lower density gasses.

In addition, the low Mach number effects are apparent in the temperature profiles. At late times, despite nearly complete combustion of the unburned gas which is releasing energy only locally at the flame front at the domain edges, the high temperature zone is located in the center of the domain. This effect is due to the uniform rise in bulk thermodynamic pressure; as the pressure rises, the temperature rises highest in the center where combustion is completed and the density is lowest.

We establish convergence rate by solving the same problem with smooth initial data on coarse and fine grids, outputting the results at a fixed time, and comparing the difference on adjacent grids. Our initial stream function is

$$\Psi^0 = \pi^{-1} \sin^2(\pi y) \sin^2(\pi x) \quad (5.1)$$

while our initial temperature and mass fraction consists of two "hot spots", one at (.25, .25) and another at (.75, .75) defined by

$$T^0 = \frac{1}{T_H} + \frac{\tanh((r - 0.125)32) + 1}{2} + \left(\frac{1}{T_L} - \frac{1}{T_H} \right) \frac{\tanh((r - 0.125)32) + 1}{2} \quad (5.2)$$

The results of the convergence study are summarized in tables 1, 2, and 3.

Acknowledgments

Research supported at the University of California, Berkeley by DARPA and the National Science Foundation under grant DMS-8919074; by a National Science Foundation Presidential Young Investigator award under grant ACS-8958522; and by the Department of Energy Office of Scientific Computing HPCC program under grant DE-FG03-92ER25140. Research supported at the Lawrence Livermore National Laboratory under the auspices of the U.S. Department of Energy under contract W-7405-Eng-48. Support under contract W-7405-Eng-48 was provided by the AMS and HPCC Programs of the DOE Office of Scientific Computing, and by the Defense Nuclear Agency under IACRO93-817.

References

1. J.B. Bell, P. Colella and H.M. Glaz, "A Second Order Projection Method for the Incompressible Navier-Stokes Equations," *J. Comp. Phys.*, v. 85, pp. 257-283, 1989.
2. J.B. Bell, P. Colella, and L.H. Howell, "An Efficient Second Order Projection Method for Viscous Incompressible Flow," *Proceedings, AIAA 10th Comp. Fluid Dynamics Conf.*, Honolulu, HI, June 24-26, pp.360-367, 1991.

- tion Method for Variable Density Flows,” *J. Comp. Phys.*, v. 101, pp. 334-348, 1992.
4. A.J. Chorin, “Numerical Solutions of the Navier-Stokes Equations,” *Math. Comp.*, v. 22, pp. 745-762, 1968.
 5. A.J. Chorin, “On the Convergence of Discrete Approximations to the Navier-Stokes Equations,” *Math. Comp.*, v. 23, pp. 341-353, 1969.
 6. F.H. Harlow and J. E. Welch, “Numerical Calculation of Time-Dependent Viscous Incompressible Flow of Fluids with Free Surfaces”, *Physics of Fluids* v. 8, pp. 2182-2189, 1965.
 7. A. Majda and J.A. Sethian, “The Derivation and Numerical Solution of the Equations for Zero Mach Number Combustion,” *Combust. Sci. Tech.*, v. 42, pp. 185-205, 1985.
 8. R. G. Rehm and H.R. Baum, “The Equations of Motion for Thermally Driven Buoyant Flow”, *Journal of Research of National Bureau of Standards*, vol. 83, no 3, 1978.
 9. J. Van Kan, “A Second-Order Accurate Pressure-Correction Scheme for Viscous Incompressible Flow,” *SIAM J. Sci. Stat. Comput.*, v. 7, no. 3, pp. 870-891, 1986.
 10. J.B. Bell and P. Colella, “A Simplified Projection Method for Incompressible Flow”, to appear.

Table 1: Velocity Convergence Results

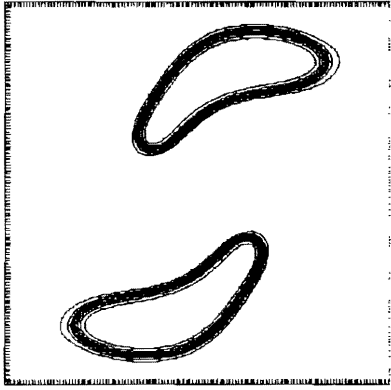
Norm	Case	32-64	Rate	64-128	Rate	128-256
L1	Euler	1.723e-02	2.17	3.669e-03	1.95	9.647e-04
	Re = 100	9.599e-03	2.07	2.255e-03	2.01	5.577e-04
L2	Euler	2.507e-02	2.14	5.479e-03	1.86	1.565e-03
	Re = 100	9.994e-03	2.07	2.236e-03	2.02	5.730e-04

Table 2: Temperature Convergence Results

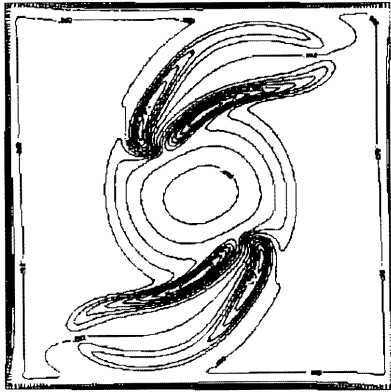
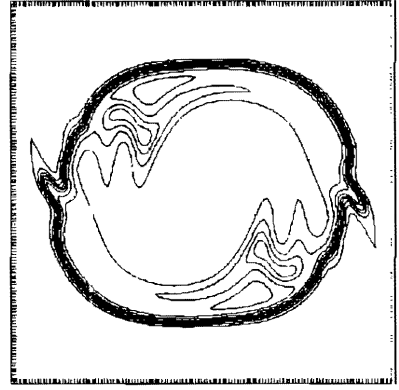
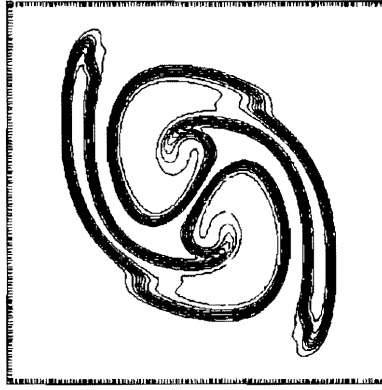
Norm	Case	32-64	Rate	64-128	Rate	128-256
L1	Pr = 0	3.111e-03	2.14	6.832e-04	2.00	1.702e-04
	Pr = 1	2.221e-03	1.98	5.651e-04	1.98	1.442e-04
L2	Pr = 0	6.612e-03	2.24	1.335e-03	2.06	3.146e-04
	Pr = 1	4.535e-03	2.08	1.045e-03	2.01	2.582e-04

Table 3: Mass Fraction Convergence Results

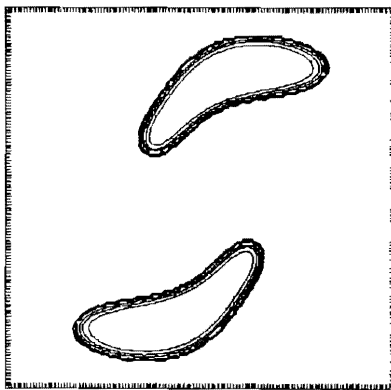
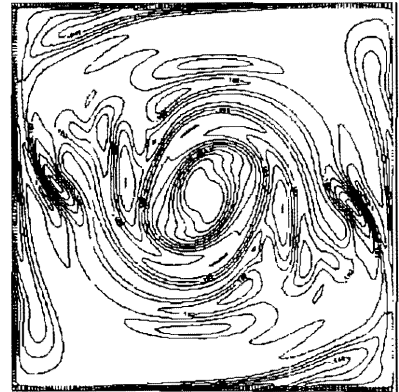
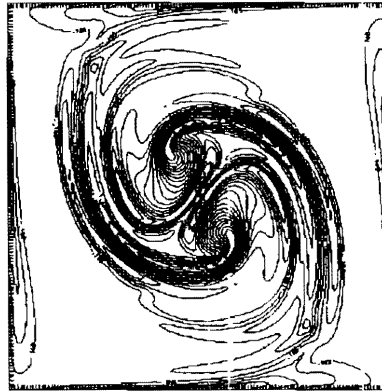
Norm	Case	32-64	Rate	64-128	Rate	128-256
L1	Sc = 0	4.436e-03	2.11	6.157e-04	1.94	1.626e-04
	Sc = 1	1.786e-03	2.02	4.395e-04	2.01	1.441e-04
L2	Sc = 0	4.793e-03	2.13	1.059e-03	1.94	2.806e-04
	Sc = 1	2.898e-03	2.06	6.858e-04	2.02	1.686e-04



Temperature Profiles



Vorticity Profiles



Location of Flame Front

